due to the distortion of the double ring.[11]

900–1200 cm^{-1}. The infrared spectrum of zeolite A shows a strong band at 995 cm^{-1}, along with weak shoulders at 1050 and 1090 cm^{-1}.[17] These bands have been assigned to T–O asymmetric stretches and are sensitive to the Si/Al ratio. The Raman spectrum of zeolite A shows three well-defined bands in this region at 972, 1050, and 1103 cm^{-1}. We have assigned these bands as arising from Si–O stretches.[11] On the basis of studies of Li^+ partially exchanging into $Na_{12}A$ and $K_{12}A$, we have proposed that these vibrations were localized on motions of the three different types of oxygen atoms in zeolite A. The bands at 972, 1050, and 1103 cm^{-1} were assigned to T–O(3), T–O(1), and T–O(2) stretching motions, respectively.[12] From No et al.'s calculations of vibrations of zeolite A,[17] it is indeed clear that such a localized motion of only one of the types of oxygen is indeed possible. They calculate a band at 1088 cm^{-1} which is characterized by the asymmetric stretch of the $Si_2Al_2(O(3))_4$ ring with no motion from the other O(1) and O(2) oxygen atoms. Examination of their normal modes also show a calculated frequency at 1134 cm^{-1}, characterized mostly by T–O(2) motion. No normal mode distinguished only by T–O(1) motion could be discerned from their study.

The change in Si/Al ratios have a complicated effect on these frequencies. At Si/Al = 1.2, only the bands at 972 and 1103 cm^{-1} are perturbed. Both these bands exhibit considerable broadening and shifts in frequency to 990 and 1110 cm^{-1}. At this stoichiometry, one of the Al atoms in each sodalite cage is replaced by a Si atom (Si-13, Al-11). The rearrangement of the Si and Al atoms in this ZK-4 structure has produced no effect on the T–O(1) vibration. As the Si/Al ratio increases to 1.4, all three bands exhibit further increases in frequency (Figure 3). At Si/Al = 2.0, the T–O(1) band splits into two bands at 1047 and 1087 cm^{-1}. Figure 4 shows a curve deconvoluted pattern in the 900–1200-cm^{-1} region for zeolites with Si/Al of 1.4, 2.0, and 2.7. Band maxima were chosen directly from the observed spectra and the widths and the intensities were varied to get the best fit to the observed data. At Si/Al = 2.7, the ~1090-cm^{-1} band decreases considerably in intensity. Examination of the intensities of the bands in the 900–1200-cm^{-1} region indicates that the high-frequency component at ~1100-cm^{-1} region gradually gains in intensity at the expense of the ~1050-cm^{-1} band as the Si/Al ratio increases. It is difficult, at present, to relate these spectral changes to structural features of zeolite A. However, it is clear that the Raman spectra are sensitive to the arrangement of the Si and Al atoms and the coupling between them. Considerably more data in the form of isotopic replacements, chemical modification, and normal-mode calculations are required before an exact correlation of the vibrational spectra and zeolitic structure can be made. However, as this study, along with the calculations of No et al., shows,[17] there is much to be gained from these continuing studies on the vibrational spectra of zeolitic crystals.

Acknowledgment. We gratefully acknowledge the support provided by the National Science Foundation (CHE-8510614). We also thank Professor J. W. Downs for the cell refinement computer program.

Absorption Spectra of Intermolecular Charge-Transfer Transitions between Xenon and Halogen Molecules (F_2, Cl_2, Br_2) in Liquid Xenon

Mario E. Fajardo, V. A. Apkarian,*

Department of Chemistry, University of California, Irvine, California 92717

Antonis Moustakas, Herman Krueger, and Eric Weitz*

Department of Chemistry, Northwestern University, Evanston, Illinois 60201 *(Received: June 16, 1987)*

The intermolecular charge-transfer transitions between molecular halogens, X_2, and Xe can be observed in UV spectra of X_2:Xe liquid solutions (X_2 = F_2, Cl_2, Br_2). In all cases the spectra occur near the UV cutoff of the spectrometer (187 nm). The absorption coefficients at 200 nm are 6.9×10^{-18}, 1.2×10^{-18}, and 2.0×10^{-17} cm^2 for Xe:F_2, Xe:Cl_2, and Xe:Br_2, respectively. Implications with respect to one-photon- and two-photon-induced cooperative photoproduction of rare gas halides in gas and condensed phases are discussed.

Introduction

Gas-phase laser-assisted reactions of halogens, X_2, with rare gas atoms, Rg, to yield the rare gas halides

$$Rg + X_2 + h\nu \rightarrow Rg^+X_2^- \rightarrow Rg^+X^- + X \qquad (1)$$

were among the first systems advanced as models for the study of radiative collisional processes[1] and were subsequently demonstrated experimentally by several groups.[1-4] Even in the case of xenon as the rare gas atom, to which all of the studies to date have been limited, the accepted thresholds for these photoinduced harpooning processes is in the vacuum-UV.

The two-photon version of the same process

$$Rg + X_2 + 2h\nu \rightarrow Rg^+X_2^- \rightarrow Rg^+X^- + X \qquad (2)$$

is then more convenient for study with readily available radiation sources and has been characterized in both bulb studies[5] and Xe:X_2 (X_2 = Cl_2 or Br_2) van der Waals complexes formed in molecular beams.[6]

(1) Yakovlenko, S. I. *Sov. J. Quantum Electron. (Engl. Transl.)* **1978**, *8*, 151. Dubov, V. A.; Gudzenko, L. I.; Gurvich, L. V.; Iakovlenko, S. I. *Chem. Phys. Lett.* **1977**, *45*, 330; **1977**, *46*, 25.

(2) Grieneisen, H. P.; Xue-Jing, Hu; Kompa, K. L. *Chem. Phys. Lett.* **1981**, *82*, 421.

(3) Dubov, V. S.; Lapsker, Ya E.; Samoilova, A. N.; Gurvich, L. V. *Chem. Phys. Lett.* **1981**, *83*, 518.

(4) Wilcomb, B. E.; Burnham, R. *J. Chem. Phys.* **1981**, *74*, 6784.

(5) Yu, Y. C.; Setser, D. W.; Horiguchi, H. *J. Phys. Chem.* **1983**, *87*, 2209. Setser, D. W.; Ku, J. In *Photophysics and Photochemistry above 6 eV*; Elsevier: New York, 1985; p 621.

(6) Boivineau, M.; Le Calve, J.; Castex, M. C.; Jouvet, C. *Chem. Phys. Lett.* **1986**, *128*, 528; *J. Chem. Phys.* **1986**, *84*, 4712.

0022-3654/88/2092-0357$01.50/0

The two-photon reaction of eq 2 for Rg = Xe and $X_2 = Cl_2$ and HCl has also been studied in rare gas matrices[7] and liquid solutions.[8] The studies have since been extended to $X_2 = F_2$, Br_2, HBr, and Rg = Xe and Kr (solid and liquid).[9] The anticipated enhanced cross sections (due to large number densities of the $Rg:X_2$ complexes) and the lowering of photon thresholds (due to solvation of the charge-transfer complex by the polarizable medium) were verified.[7,8] The condensed-phase studies are particularly interesting since they provide a means of studying many-body dynamics. Moreover, due to the large exciplex densities created in these processes, the mechanisms of eq 1 and 2 may serve as a general scheme for optically pumped condensed-phase exciplex lasers.[10]

A knowledge of the optical threshold for these charge-transfer transitions is obviously of great interest. In the past this has been estimated based on theoretical grounds. The simplicity of the system clearly yields itself to reliable estimates. Yet there is wide discrepancy between the observed and rationalized thresholds. To estimate the threshold wavelengths for these cooperative transitions, a knowledge of the vertical electron affinities of the halogens is necessary. The most reliable source of vertical electron affinities is charge-transfer absorptions in electron-donating solvents.[11] Such studies were initiated by Mulliken[12] and have been recently revised to produce the most complete set of X_2^- potentials.[13]

The charge-transfer transitions between xenon and molecular halogens can be directly observed in UV absorption spectra of X_2:Xe solutions. These spectra are presented and discussed in this report. Their relevance to the condensed-phase studies is direct; the data also shed light on the gas-phase studies. Extension of these studies to the vacuum-UV could provide the clearest source of X_2^- ground- and excited-state potentials.

Experimental Section

Spectra were recorded with a Perkin-Elmer 330 UV–vis spectrometer with a UV cutoff at 187 nm. The onset of atmospheric absorptions results in a usable spectral region extending down to approximately 195 nm.

The following gases, with their stated purities, were used without further purification: xenon (Cryogenic Rare Gas, Research Grade), 99.995%; chlorine (Matheson, Research Grade), 99.96%; 10% fluorine in helium (Spectra Gases). In addition, bromine (Aesar, 99.9%) was subjected to one vacuum distillation over barium oxide.

The solutions were prepared in a high-pressure cryocell kept at 205 K; the design of the cell has been previously described.[14] For Cl_2 and F_2, rare gas solutions were prepared as described in ref 14. In the case of F_2, the vacuum system and cell were passivated by overnight exposure to approximately 500 Torr of the F_2–He mixture. Because of the low vapor pressure of bromine near 205 K, Br_2–liquid xenon solutions were prepared in a different manner. The cell was first partially filled with liquid xenon, after which a fixed volume of a gaseous Br_2–Xe mixture of known Br_2 concentration was admitted. Finally, the remaining volume of the cell was filled with liquid xenon.

Absorption spectra of the halogens were recorded both in the gas phase and in liquid xenon solution. Concentrations of gas-phase samples were calculated simply from the cell temperature (205 K) and the sample pressure, as determined with an MKS Baratron. Prior to scans of halogen–liquid xenon solutions, a scan of pure liquid xenon was obtained to serve as a background.

The major source of error in the reported solution-phase cross sections involves determining the halogen concentration in liquid xenon. This is due to the fact that a fraction of the halogen molecules added to the cell in the course of sample preparation adsorb on the cell walls as evidenced by a gradual drop in halogen pressure with time. When liquid xenon is added to the cell, some adsorbed halogen molecules may dissolve along with those that were in the gas phase. Considering the relatively low concentrations employed in the present experiments (as necessitated by the relatively large cross sections measured), dissolution of adsorbed species may be significant.

Since both Br_2 and Cl_2 possess molecular absorptions in the visible (peaking around 420 and 330 nm, respectively)[15] which are sufficiently strong to be observed at the solution concentrations employed, a knowledge of the cross sections for these transitions could be used to determine accurate solution-phase concentrations. To a first approximation, the gas-phase cross sections for Br_2 and Cl_2 can be employed. However, the gas-phase cross sections would only be expected to approximate the actual solution-phase cross sections. Minimally, it would be expected that the solution-phase cross section would differ from the gas phase due to the differences in dielectric constant of the medium. The nature of the correction term is of the well-known form[16]

$$\frac{1}{n}\left[\frac{n^2+2}{3}\right]^2$$

where n is the index of refraction of the medium. For liquid xenon this predicts an enhancement of 22% in the absorption cross section versus the gas phase.

Obviously, an exact determination of the solution-phase visible cross section requires an exact knowledge of the solution-phase concentration of the halogen which is fraught with the previously indicated problems. Nevertheless, more accurate measurements of concentrations can be made for more concentrated solutions. This has been done for Cl_2, and the peak extinction coefficient of the visible absorption of Cl_2 in liquid Xe (at 327 nm) is found to increase by 35%, versus the gas phase. This measured liquid-phase cross section is thus within ~10% of that predicted by simply multiplying the gas-phase cross section by the dielectric correction.

Thus, the Cl_2 and Br_2 concentrations used in calculating solution-phase cross sections at 200 nm were determined by using the intensity of the visible transitions in the liquid phase and reported *gas-phase* cross sections for these transitions corrected for the dielectric effect of liquid Xe. This procedure is expected to produce a lower limit for the reported 200-nm solution-phase cross section.

Fluorine possesses a weak molecular absorption near 300 nm. At the concentrations of F_2 employed in this study, the strength of this transition is not accurately measurable. Thus, the concentration of F_2 in F_2–liquid xenon solution was estimated based on the pressure of F_2–He mixture used. Assuming complete passivation of the cell and complete solubility of all gas-phase F_2, one obtains an *upper limit* for the 200-nm cross section of F_2 in liquid xenon using this concentration.

Results and Discussion

Spectra of X_2 and X_2:Xe solutions ($X_2 = F_2$, Cl_2, Br_2) are collected in Figure 1. In all cases, upon addition of xenon a very intense absorption is observed near the UV limit of the spectrometer (upper traces in Figure 1). The fact that this asorption is absent in the halogens and that there are no xenon absorptions in this spectral range clearly establishes that the absorption is due to an intermolecular transition between X_2 and Xe. Since in none of the cases is it clear that the absorption maximum is observed, we report the absorption cross sections at 200 nm. They are 6.9

(7) Fajardo, M. E.; Apkarian, V. A. *J. Chem. Phys.* **1986**, *85*, 5660; *Chem. Phys. Lett.* **1987**, *134*, 51.
(8) Wiedeman, L.; Fajardo, M. E.; Apkarian, V. A. *Chem. Phys. Lett.* **1987**, *134*, 55.
(9) Fajardo, M. E.; Wiedeman, L.; Apkarian, V. A.; submitted for publication in *J. Phys. Chem.*
(10) Shahid, M.; Jara, H.; Pummer, H.; Egger, H.; Rhodes, C. K. *Opt. Lett.* **1985**, *10*, 448.
(11) Person, W. B. *J. Chem. Phys.* **1963**, *38*, 109.
(12) Mulliken, R. S. *J. Am. Chem. Soc.* **1950**, *74*, 600, 811; *J. Phys. Chem.* **1952**, *56*, 801.
(13) Chen, E. C. M.; Wentworth, W. E. *J. Phys. Chem.* **1985**, *89*, 4099 and references therein.
(14) Knudtson, J. T.; Weitz, E. *Chem. Phys. Lett.* **1984**, *104*, 71.
(15) *Photochemistry of Small Molecules*; Okabe, H., Ed.; Wiley: New York, 1978.
(16) Knudtson, J. T.; Weitz, E. *J. Chem. Phys.* **1985**, *83*, 927.

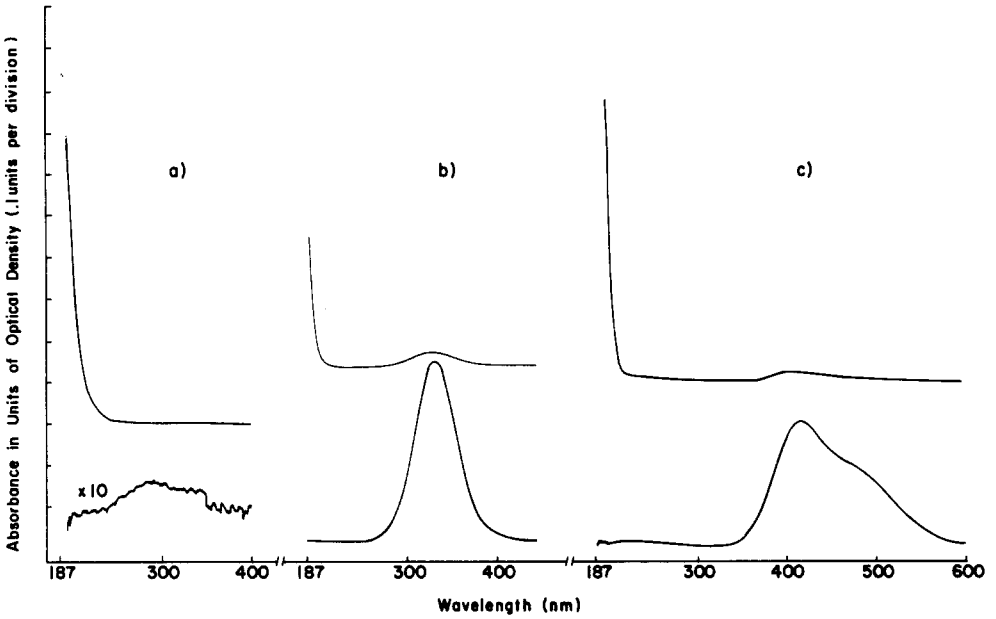

Figure 1. UV–vis spectra of F_2 (a), Cl_2 (b), and Br_2 (c) in liquid xenon solution (upper traces) and in the gas phase (lower traces). Gas-phase concentrations are 1.8×10^{17}, 1.0×10^{18}, and 4.2×10^{17} molecules/cm^3 for F_2, Cl_2, and Br_2, respectively. Solution-phase concentrations are estimated (see text) to be 4.5×10^{16}, 5.3×10^{16}, and 1.4×10^{16} molecules/cm^3 for F_2, Cl_2, and Br_2. The cell path length is 3.81 cm.

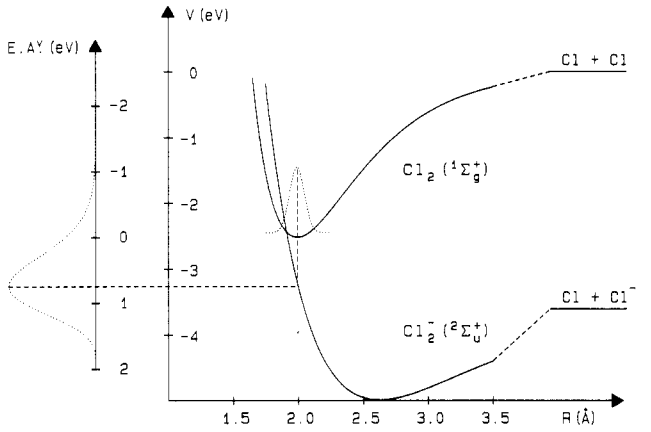

Figure 2. $Cl_2(^1\Sigma_g^+)$ and $Cl_2^-(^2\Sigma_u^+)$ potentials according to Chen and Wentworth (ref 13) are shown. The vertical electron affinity from $v = 0$ of Cl_2 obtained in the reflection approximation is shown along the ordinate.

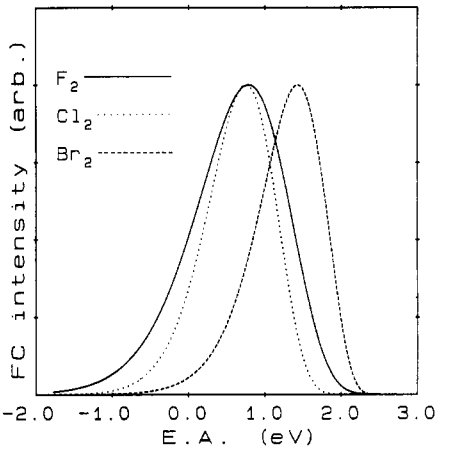

Figure 3. Vertical electron affinities of F_2, Cl_2, and Br_2. The ordinate corresponds to the Franck–Condon intensities (probabilities), normalized to the same height.

$\times 10^{-18}$, 1.2×10^{-18}, and 2.0×10^{-17} cm^2 for Xe:F_2, Xe:Cl_2, and Xe:Br_2, respectively. Such intense absorptions are characteristic of charge-transfer transitions. It can be safely assumed that the observed portion of the spectrum is at best half the entire band; thus, lower limits on oscillator strengths can be established as

$$f \gtrsim 1.202 \times 10^{12} \sigma_{max} \left(\frac{\Delta\lambda}{\lambda_{max}^2} \right) \quad (3)$$

in which $\Delta\lambda$ corresponds to the full width at half-maximum (2 $\times$ hwhm). It can then be estimated that $f \gtrsim 0.01$, 0.017, and 0.05 for Xe:F_2, Xe:Cl_2, and Xe:Br_2, respectively. For a single-electron transition in which a full charge is transferred an oscillator strength of near unity is to be expected. It is then difficult to establish whether the true maximum is observed in any of the spectra based on the estimated minimal oscillator strengths.

We may estimate the maxima in these charge-transfer transitions and their expected minimal widths based on simple arguments. For a Xe:X_2 pair at contact distance r_c, the optical transition energy is given as

$$E_{h\nu}(r_c) = \mathrm{IP(Xe)} - \mathrm{EA^v}(X_2) + \Delta V(r_c) \quad (4)$$

in which $EA^v(X_2)$ is the vertical electron affinity of the molecular halogen and $\Delta V(r_c)$ is the difference in ionic excited-state and neutral ground-state potentials.

The vertical electron affinities of all molecular halogens are broad, since the $v = 0$ of the neutral ground state $X_2(\Sigma_g^+)$ maps out the repulsive wall of the negative ion ground state, $X_2^-(^2\Sigma_u^+)$. The pertinent potentials for Cl_2, taken from ref 13, are shown in Figure 2. The vertical electron affinity distribution, calculated as a reflection of the $v = 0$ harmonic wave function on the $^2\Sigma_u^+$ potential, is shown along the ordinate. The calculated electron affinities of all three halogens by the same method, however, including all thermally populated states at 200 K are shown in Figure 3. In all cases both negative and positive electron affinities are possible due to the crossing of the X_2^- repulsive wall with the $v = 0$ wave function in X_2. The breadths of these distributions are mainly a reflection of the steepness of the X_2^- repulsive wall.

The last term in eq 4 is the difference between excited state and ground state of the pair at contact. The ground state can be calculated as a sum of pairwise additive contributions in the liquid phase. The upper state is dominated by the Coulombic interaction between the charged pair; however, a contribution due to Cl_2^-–Xe and Xe^+–Xe van der Waals potentials is also present. Little error is made by ignoring the van der Waals energies in both states since they nearly cancel each other and individually

TABLE I: Charge-Transfer Absorption Maxima for Xe + X_2 + $h\nu$ → $Xe^+X_2^-$

atoms	r,[a] Å	r_c,[b] Å	e^2/r, eV	EA^v_{max}	$e^2(\epsilon - 1)/[(2\epsilon + 1)r_c]$[d]	λ, nm
F	1.55	3.55	4.05	0.8	0.69	188
Cl	1.75	3.75	3.85	0.75	0.65	180
Br	1.9	3.9	3.7	1.5	0.63	197
Xe	2.0					

[a] Van der Waals atomic radii. [b] Contact distance. [c] Maxima of electron affinity distributions (see Figure 2). [d] $\epsilon = n^2$; $n = 1.33$ for liquid xenon at 200 K, calculated from the known saturated liquid density of xenon at 200 K.

they are a minor contribution to the overall energies.[17] Thus, $\Delta V(r_c)$ can be reduced to

$$\Delta V(r_c) = V(Xe^+X_2^-)r_c = -\frac{e^2}{r_c} - \frac{8(\epsilon - 1)}{(2\epsilon + 1)}\frac{\mu^2}{d^3} \quad (5)$$

in which only the Coulombic attraction between Xe^+ and X_2^- and the solvation of the $Xe^+X_2^-$ dipole in a continuum dielectric are retained (d = cavity diameter, μ = molecular dipole). If we further make the assumption that $d = 2r_c$ and that $\mu = er_c$, $\Delta V(r_c)$ can be estimated. Using for r_c the sum of van der Waals radii, we can calculate $E_{h\nu}$ of eq 4. These estimates are collected in Table I.

The agreement between estimated maxima and the observed spectra is acceptable given the very crude approximations that were made. The UV cutoff of the spectrometer is predicted to be very near the band maxima. The true bandwidths should be as large as the vertical electron affinity distributions, ~4 eV in the case of $Xe^+F_2^-$. There should be further broadening on the blue edge due to the distribution of Xe–X_2 distances. A convolution of $E(r_c)$ of eq 4 over the X_2–Xe radial distribution, weighted by the distance-dependent transition dipole, is the most appropriate representation of the experimental line shape. In the absence of a more complete spectrum such a treatment is not warranted.

The observation of these contact charge-transfer absorption thresholds and a knowledge of their expected minimal widths have significant implications with respect to photoinduced exciplex formation in condensed phases, in the gas phase, and in X_2:Rg complexes or clusters.[1-10] The implications with respect to liquid-phase exciplex formation is obvious. All halogens in liquid xenon could be pumped efficiently at 193 nm to generate rare gas halides by the one-photon harpooning mechanism of eq 1. For rare gases other than Xe, the absorption bands can be predicted to be shifted mainly by the difference in ionization potentials. For the case of two-photon pumping, eq 2, it can be predicted that the xenon halides can be generated in liquid xenon at wavelengths as long as ~400 nm. This prediction has already been verified.[9]

The interpretation of two-photon-induced cooperative absorptions requires a consideration of intermediate-state resonances as well as the final charge-transfer state. In the gas phase, Setser and co-workers have reported a threshold near 360 nm for Xe + Cl_2 + $2h\nu \rightarrow Xe^+Cl_2^-$, while in the case of Xe + Br_2 + $2h\nu \rightarrow Xe^+Br_2^-$, a threshold near 280 nm was observed.[5] These results were corroborated by the beam experiments.[6] This represents an apparent contradiction with the present data which suggests that the charge-transfer transitions for all Xe:X_2 should overlap and the $Xe^+Br_2^-$ threshold should be slightly lower than that of $Xe^+Cl_2^-$. This apparent discrepancy can be rationalized as due to the fact that, in the case of Cl_2, the two-photon transition has a real intermediate resonance, namely the $Cl_2(^1\Pi,^3\Pi)$ repulsive potentials which give rise to the molecular absorption at 330 nm. Furthermore, if this intermediate state of the complex is regarded as $Xe(^1S):Cl(^2P):Cl(^2P)$, then the second photon is resonant with the diatomic exciplex transitions $Xe^+Cl^-(B/C):Cl(^2P) \leftarrow XeCl(A/X):Cl(^2P)$. Thus, the two-photon charge-transfer transition of Xe:Cl_2 complexes is enhanced by resonances for both photons:

$$Xe(^1S_0) + Cl_2(^1\Sigma_g^+) \xrightarrow{h\nu} [Xe(^1S_0) + Cl_2(^1\Pi,^3\Pi) = Xe(^1S_0) + Cl(^2P) + Cl(^2P)] \xrightarrow{h\nu} Xe^+Cl^-(B,C) + Cl(^2P) \quad (6)$$

The same resonance is not available for the case of Xe + Br_2 + $2h\nu$. The molecular absorption is at 420 nm, while the diatomic exciplex transition is near 280 nm. The observed threshold does correspond to a resonance in the second photon absorption in the scheme of eq 6. These arguments imply that the reported thresholds for the gas-phase observations of these transitions are detection thresholds and not energetic ones.

Conclusions

Intense charge-transfer transitions between xenon and X_2 (X_2 = F_2, Cl_2, Br_2) are observed in X_2:Xe solutions. These absorptions occur near the UV cutoff of our spectrometer; nevertheless, it is believed that the absorption maxima are near this cutoff (~187 nm). The peak positions are justified based on solvation of the charge-transfer complex in the polarizable liquid. It is, however, clear that due to the broad distribution of electron affinities, the charge-transfer bands of all $Rg^+X_2^- \leftarrow RgX_2$ absorptions overlap. Since the solvation energies of all $Rg^+X_2^-$ complexes in a given solvent are similar (~0.5 eV for Xe), the latter conclusion should hold for the gas phase also. Extended vacuum-UV spectra of these solutions would be indeed useful for the determination of to X_2^- ground and excited potentials. Due to the simplicity of the atomic solvents, rigorous analysis of such spectra via radial distribution functions should be possible. The latter would yield the effective many-body Rg–X_2 intermolecular potentials. The same absorptions should be detectable in the gas phase since a large fraction of the halogens in X_2:Xe mixtures should be complexed.

Acknowledgment. This research was supported in part by the United States Air Force Astronautics Laboratory under Contract FO4611-87-K-0024 (V.A.A.) and by the National Science Foundation under Grant CHE 85-06957 (E.W.).

Registry No. Xe, 7440-63-3; F_2, 7782-41-4; Cl_2, 7782-50-5; Br_2, 7726-95-6.

(17) For a more detailed analysis, see the related calculation for $Xe_2^+Cl^-$ in condensed xenon by Last and George (Last, I.; George, T. F. *J. Chem. Phys.* **1987**, *86*, 3787).